Microbial oxidation as a methane sink beneath the West Antarctic Ice Sheet

Michaud, Alexander B.; Dore, John E.; Achberger, Amanda M.; Christner, Brent C.; Mitchell, Andrew; Skidmore, Mark L.; Vick-Majors, Trista; Priscu, John C.

Published in:
Nature Geoscience

DOI:
10.1038/ngeo2992

Publication date:
2017

Citation for published version (APA):
Michaud, A. B., Dore, J. E., Achberger, A. M., Christner, B. C., Mitchell, A., Skidmore, M. L., Vick-Majors, T., & Priscu, J. C. (2017). Microbial oxidation as a methane sink beneath the West Antarctic Ice Sheet. *Nature Geoscience*, *10*, 582-586. https://doi.org/10.1038/ngeo2992

Microbial oxidation as a methane sink beneath the West Antarctic Ice Sheet

Alexander B. Michaud[1,†,*], John E. Dore[1], Amanda M. Achberger[2,‡], Brent C. Christner[2,3], Andrew C. Mitchell[4], Mark L. Skidmore[5], Trista J. Vick-Majors[1,††], and John C. Priscu[1,*]

[1] Department of Land Resources and Environmental Sciences, Montana State University, Bozeman, MT, 59717, USA

[2] Department of Biological Sciences, Louisiana State University, Baton Rouge, LA, 70803, USA

[3] Department of Microbiology and Cell Science, University of Florida, Gainesville, FL, 32611, USA

[4] Department of Geography and Earth Sciences, Aberystwyth University, Aberystwyth, SY23 3DB, UK

[5] Department of Earth Sciences, Montana State University, Bozeman, MT, 59717, USA

[*] Correspondence to: John C. Priscu, jpriscu@montana.edu or Alexander B. Michaud, abmichaud@gmail.com

[†] Present Address: Center for Geomicrobiology, Department of Bioscience, Aarhus University, 8000 Aarhus C, DK

[‡] Present Address: Department of Oceanography, Texas A&M University, College Station, TX, 77840, USA

[††] Present Address: Département des Sciences Biologiques, Université du Québec à Montréal, Case Postale 8888, Succursale Centre-Ville, Montréal, Quebec, Canada H3C 3P8

Summary Paragraph

Aquatic habitats beneath ice masses contain active microbial ecosystems capable of cycling important greenhouse gases, such as methane (CH_4). Models suggest that a large methane reservoir exists beneath the West Antarctic Ice Sheet, but the quantity, source and fate of such methane remain poorly understood. The availability of O_2 from basal melting of the West Antarctic Ice Sheet provides conditions favorable for aerobic methane oxidation. Here, we present measurements of methane concentration and stable isotopic composition from Subglacial Lake Whillans, which lies beneath the West Antarctic Ice Sheet. We show that sub-ice sheet methane is produced through the biological reduction of carbon dioxide using H_2. This methane pool is subsequently consumed by aerobic, bacterial methane oxidation at the lake sediment-water interface, a metabolic process supported by the presence of genes involved in methane oxidation. Bacterial oxidation consumes >99% of the methane and represents a significant methane sink, and source of biomass carbon and metabolic energy to the surficial SLW sediments. Our data reveal that aerobic methanotrophy may mitigate the release of methane to the atmosphere during subglacial water drainage to ice sheet margins and during periods of deglaciation.

Main Text

Methane (CH_4) is an important greenhouse gas that affects atmospheric chemistry and radiative balance of Earth. Consequently, understanding its global sources, sinks, and feedbacks within the climate system is of considerable importance[1]. The primary pathway for biological CH_4 production in carbon-rich habitats (e.g., bogs, wetlands) is the anaerobic fermentation of simple organic compounds by certain archaea (acetoclastic or methylotrophic methanogenesis[2]).

An alternative microbial pathway to CH_4 production is the reduction of CO_2 coupled to the oxidation of H_2 (hydrogenotrophic methanogenesis), which is common in anoxic, low sulfate environments such as the methanogenic zone within marine sediments[2]. Conversely, bacterial and archaeal oxidation of CH_4 (aerobic and anaerobic, respectively) to CO_2 is a major pathway that reduces net CH_4 release to the atmosphere[3].

Anoxic habitats in sediments beneath the Antarctic ice sheet may be globally important sites of biological CH_4 production that could potentially add significant CH_4 to the atmosphere upon subglacial water drainage to the ice sheet margins or deglaciation[4–6]. However, due to release of oxygen into the subglacial environment from the overlying ice sheet through geothermal heat-induced melting[7–9], aerobic methanotrophic activity can ultimately mitigate CH_4 release to the atmosphere. We present the first data on CH_4 concentration and stable isotopic composition, along with genomic data collected from Subglacial Lake Whillans (SLW), which lies ~800 m beneath the West Antarctic Ice Sheet (WAIS). Collectively, these data reveal the presence of an ecosystem supported, in part, by active microbial transformations of CH_4.

Quantity and source of sub ice-sheet CH_4. CH_4 concentration in SLW ranged from 0.024 μM in the lake water to 300 μM in the deepest (39 cm) sediment porewater sample (Fig. 1). Fick's first law was used to compute a flux of 6.8 ± 1.8 (mean ± SE) mmol CH_4 m^{-2} y^{-1} into the surficial sediment (0-2 cm) of SLW using the concentration gradient in the top 15 cm of sediment and the associated error of the concentration gradient, which includes any potential sampling artifacts. CH_4 in the SLW sediment had an average $\delta^{13}C$-CH_4 value of -74.7‰ (range: -77.1 to -70.1‰) (Fig. 1) and, together with δD-CH_4 values (range: -247.6 to -239.3‰), reveals that SLW CH_4 is likely produced by hydrogenotrophic methanogenesis[10] (Fig. 2). This conclusion contrasts with previous models suggesting that potential CH_4 reservoirs beneath the

WAIS would be largely formed through acetoclastic methanogenesis[4]. Hydrogenotrophic methanogenesis is common in marine sediments and other environments with low concentrations of old organic carbon, supporting our results from SLW, which also has low organic carbon and acetate (2-14 μM) relative to environments with active acetoclastic methanogenesis[10–13] (Supplementary Fig. 1). CO_2 for hydrogenotrophic methanogenesis can be supplied from microbial respiration or bicarbonate in sediment porewater (2-6 mM)[14], and hydrogen can be generated abiotically from glacially-crushed siliceous bedrock, radiolysis of water, hydrothermal input, or biologically via fermentation[2,8,15,16]. Attempts to amplify a marker gene for methanogenic archaea (*mcrA*)[17,18] from the 0-2, 4-6, 18-20 and 34-36 cm depth intervals within the SLW sediment core were unsuccessful, implying that the abundance of methanogenic archaea was low or below detection. A community analysis of 16S rRNA molecules, which indicates the potentially active fraction of the microbial community[19,20], showed relatives of methanogenic species (i.e., *Methanohalophilus levihalophilus*) were rare members (0.1%) of the active sediment community at 35 cm depth (Fig. 1B)[21]. The most parsimonious explanation for our concentration profile and molecular microbiological results is the presence of a contemporary or relict CH_4 source that originates from depths below our deepest sample and diffuses towards an aerobic methanotrophic sink at the sediment-water interface.

Active aerobic methanotrophy. The low water column CH_4 concentration, relative to the sediment porewater, and the decrease in CH_4 concentration in the upper ~16 cm of sediment indicate that CH_4 oxidation consumes almost all (>99%) of the upwardly diffusing sedimentary CH_4 (Fig. 1A). The four order of magnitude decrease in CH_4 concentration from the surficial sediments to the water column corresponds with a large, positive shift (30.7‰) in the $\delta^{13}C$-CH_4 (Fig. 1A). We used the Rayleigh distillation model to calculate a kinetic isotope fractionation

96 factor (KIFF) of $\alpha = 1.004$ associated with the CH_4 oxidation process[22]. This model assumes a
97 closed system (i.e., no other inputs of CH_4 and measured isotope values are not affected by
98 mixing) and that the only sink for sediment CH_4 is bacterial oxidation. The KIFF calculated for
99 CH_4 oxidation in SLW is within the lower range of those derived from laboratory cultures, but is
100 similar to estimates from field measurements made in cold, marine habitats ($\alpha = 1.003 –$
101 1.035)[22,23]. The observed fractionation in SLW is consistent with near-complete removal of
102 upwardly diffusing sedimentary CH_4 by aerobic CH_4 oxidizing bacteria[23].

103 We amplified the β-subunit of the particulate methane monooxygenase gene (*pmoA*)
104 found in aerobic CH_4 oxidizing bacteria to further evaluate the functional potential for CH_4
105 oxidation. Results revealed that *pmoA* was detectable in the water column and the upper 16 cm
106 of sediment, but not in deeper layers of the core. The presence of *pmoA* genes is consistent with
107 measured O_2 concentration of 71.9 μM, in SLW lake waters[1], and redox-sensitive trace metal
108 abundance in the sediment core that implies the presence of O_2 to a depth of ~16 cm[14]. Thus, the
109 functional potential for aerobic methanotrophy (*pmoA* gene presence) occurs where both CH_4
110 and O_2 are available. SLW *pmoA* sequences were similar (>87% DNA similarity) to
111 *Methylobacter tundripaludum*, an aerobic CH_4 oxidizing bacterium (Fig. 3). *M. tundripaludum*
112 was also the closest described and cultured phylogenetic relative (99% rDNA gene sequence
113 similarity) to the putative CH_4 oxidizing taxa recovered from 16S rDNA gene sequence analysis
114 of the SLW microbial community (Fig. 3; OTU 000112)[7,21]. The *pmoA* sequences present in
115 SLW were related to *pmoA* sequences collected from an active CH_4 oxidizing environment at the
116 margin of the Greenland Ice Sheet (Fig. 3)[5]. Although the *pmoA* primer set we used was
117 designed to detect a wide diversity of methanotrophs[24], additional putative methanotrophic

genera were detected in the 16S rDNA and rRNA community analysis (Supplementary Fig. 1), but these genera were at least one order of magnitude less abundant than *M. tundripaludum*.

Aerobic CH_4 oxidizing bacteria are typically members of the *Gammaproteobacteria* and *Alphaproteobacteria*[25] and further classified into different types based on the substrate affinity of their methane monooxygenase enzyme[25]. Type Ia *Gammaproteobacteria* methanotrophs have methane monooxygenase enzymes with low affinity for CH_4 while type II *Alphaproteobacteria* have enzymes with a high affinity for CH_4[26]. These type Ia *Gammaproteobacteria* methanotrophs, particularly *Methylobacter* sp., dominate the active fraction of methanotroph populations in freshwater environments that have high CH_4 (μM – mM) concentrations and strong CH_4 sources[25,26]. *M. tundripaludum* possesses a low affinity (type Ia) methane monooxygenase enzyme, is known to be cold-adapted[24,26], has been shown to be active at the Greenland Ice Sheet margin[5] and is responsible for significant CH_4 consumption in a variety of other Arctic habitats[27–29]. Both the low CH_4 affinity and temperature adaptation of the type Ia *Gammaproteobacteria* particulate methane monoxygenase enzyme reflect the conditions measured in SLW (-0.5°C and 0.1 to 0.3 mM CH_4; Fig. 1)[9]. Indeed, a community analysis of 16S rRNA molecules showed *M. tundripaludum* and other methanotrophic taxa were abundant (≥1.0%) in the water column and upper sediments (0-6 cm), with their greatest relative abundance in the surficial sediments (16%; Fig. 1B; Supplementary Fig. 1)[21]. These molecular data, based on *pmoA* gene sequences and 16S rRNA molecules, indicate that methanotrophs related to *M. tundripaludum* are abundant and potentially metabolically active near the SLW sediment-water interface, where geochemical data indicate peak methane oxidation.

The role of CH_4 in the subglacial ecosystem. We computed chemical affinity (A_r) for the surficial (0-2 cm) sediment layer to estimate the available biochemical energy from CH_4

oxidation compared to other potential metabolic reactions[30,31] (Fig. 4). O_2 concentration data in the surficial sediment layer are not available, so biochemical reactions were modeled at half (36.5 μM) and one-tenth (7.3 μM) of the average SLW water column O_2 concentration. These modeled O_2 concentrations are reasonable given the evidence for O_2 penetration to ~16 cm[14]. While pyrite and ammonium oxidation are predicted to yield the greatest metabolic energy in the water column[32], aerobic CH_4 oxidation is the most exergonic biochemical pathway in the surficial sediment despite the modeled 10-fold reduction in O_2 concentration relative to lake water (A_r^{e-}: 99.9 kJ mol $e^{-\ -1}$; A_r^{kg}: 2.84 J kg H_2O^{-1}) (Fig. 4). The microbial community composition reflects the chemical affinity calculations such that iron, sulfide and ammonium oxidizing taxa are abundant in the water column[21,32] and aerobic methane oxidizing taxa are abundant and active in the surficial sediment (Fig. 1). These chemical affinity calculations corroborate the molecular and geochemical data by showing sufficient biochemical energy is present in the SLW surficial sediment to support the abundant methanotroph population (Fig. 4).

We modeled the rate of biological CH_4 consumption in SLW as;

$$\frac{dC}{dt} = (F_{diff} \times A) - (R \times V) \quad (1)$$

where, $\frac{dC}{dt}$ is the change in CH_4 concentration over time, F_{diff} is the diffusional flux into the 0-2 cm surficial sediment, A is the area of SLW, R is the rate of CH_4 consumption, and V is volume of SLW plus the porewater surficial sediment. Assuming steady-state conditions (i.e., $\frac{dC}{dt} = 0$), equation (1) can be rewritten as:

$$R = \frac{F_{diff}}{H_L + (H_{SS} \times \varphi)} \quad (2)$$

where, H_L and H_{SS} are the height of the lake and surficial (0-2 cm) sediments, respectively, and φ is the sediment porosity. R equates to 3.0 ± 0.8 mmol CH_4 m^{-3} y^{-1}. The rate of CH_4 removal (R)

is the sum of both CH_4 oxidation (R_{ox}) and incorporation of CH_4 as a carbon source (R_{incorp}) for microbial biomass synthesis. Using the total CH_4 removal rate (R), together with the average fraction of CH_4 (~0.5) partitioned to biomass formation for type I methanotrophs[33], reveals that methanotrophs may oxidize 1.5 mmol CH_4 m^{-3} y^{-1} to CO_2 (R_{ox}) and assimilate 1.5 mmol CH_4 m^{-3} y^{-1} (R_{incorp}) as a biosynthetic carbon source (Supplementary Table 1). Given 0.5 as a biomass partitioning factor, the rate of aerobic CH_4 oxidation would be 10 to 100-fold lower than aerobic CH_4 oxidation measured in cold (~4°C), surficial marine sediments and deep sea, CH_4 seeps[34,35]. The biomass partitioning factor can vary from 0.06 to 0.7 in lakes with active methanotrophy[36]. When we account for this potential variability in the biomass partitioning factor and the uncertainty in the CH_4 flux, R_{ox} and R_{incorp} vary by an order of magnitude; the range of R_{incorp} is 0.14 – 3.0 mmol CH_4 m^{-3} y^{-1} and the R_{ox} is 0.52 – 3.6 mmol CH_4 m^{-3} y^{-1} (Supplementary Table 1). It is important to note that R_{ox} and R_{incorp} are inversely related (Supplementary Table 1). While the overall rate of oxidation may be low compared to marine sediment methanotrophy, if the formation of biomass due to CH_4 oxidation occurred solely in the surficial SLW sediment porewaters, where molecular data indicate peak active methanotroph abundance (Fig. 1B), the biosynthetic rate would be 26.2 ng C (L porewater)$^{-1}$ d^{-1} (range: 2.3 – 51 ng C (L porewater)$^{-1}$ d^{-1}; Supplementary Table 1). This modeled biomass C production rate via sedimentary methanotrophy is nearly equivalent (80%; range: 7 - 155%) to measured rates of chemoautotrophic biomass C production (32.9 ng C L^{-1} d^{-1}) within the SLW water column[7]. These results indicate that CH_4, as modeled, is an important carbon and energy source for the SLW sediment microbial community.

The O_2 demand derived from the modeled CH_4 removal rate (R) is 6.1 x 10^5 mol O_2 y^{-1}, using 0.5 as the biomass partitioning factor. Methanotrophy in SLW is responsible for

consuming ~16% (range: 10 – 24%; Supplementary Table 1) of the O_2 supply to the SLW ecosystem[32]. Thus, the impact of oxygen demand due to CH_4 oxidation in the SLW ecosystem depends on the balance between methanotroph growth and energy requirements. Despite a potentially large range in the biomass partitioning factor, these calculations show that O_2 released from basal melting of the overlying ice sheet fuels an abundant and active population of methanotrophs in the lake. Saturated sediments at SLW are similar in nature to those found beneath other ice streams of the Siple coast region (e.g., ref. 8) and basal ice melt is extensive beneath the WAIS[37,38], which may produce extensive oxic subglacial aquatic habitats, conducive to cosmopolitan populations of methanotrophs that convert CH_4 to CO_2 and biomass.

Our data reveal that hydrogenotrophic methanogenesis is the main pathway of CH_4 formation beneath SLW and that CH_4 is utilized by aerobic methanotrophic bacteria. Contrary to previous predictions which suggested the potential significance of subglacial CH_4 fluxes to the atmosphere (e.g., ref. 4), our CH_4 measurements and flux calculations show that aerobic methanotrophic bacteria in SLW convert most (>99%) of the sedimentary CH_4 efflux to CO_2 and biomass. The bacterial conversion of CH_4 to CO_2 beneath the WAIS reduces the warming potential of subglacial gases[39] that may be released to downstream ice sheet margin environments and to the atmosphere during episodes of ice sheet retreat. Given the potential for widespread hydrogenotrophic CH_4 production in sediments beneath ice sheets, such as the WAIS, and the release of O_2 due to melting at the ice sheet base[9,37,38], biological transformations of CH_4 may be significant for the functioning and persistence of deep microbial life and biogeochemical processes in Antarctic sub-ice environments.

References

1. Kirschke, S. *et al.* Three decades of global methane sources and sinks. *Nat. Geosci.* **6,** 813–823 (2013).
2. Thauer, R. K., Kaster, A.-K., Seedorf, H., Buckel, W. & Hedderich, R. Methanogenic archaea: ecologically relevant differences in energy conservation. *Nat. Rev. Microbiol.* **6,** 579–91 (2008).
3. Conrad, R. The global methane cycle: recent advances in understanding the microbial processes involved. *Environ. Microbiol. Rep.* **1,** 285–92 (2009).
4. Wadham, J. L. *et al.* Potential methane reservoirs beneath Antarctica. *Nature* **488,** 633–637 (2012).
5. Dieser, M. *et al.* Molecular and biogeochemical evidence for methane cycling beneath the western margin of the Greenland Ice Sheet. *ISME J.* **8,** 2305–2316 (2014).
6. Wadham, J. L. *et al.* The potential role of the Antarctic Ice Sheet in global biogeochemical cycles. *Earth Environ. Sci. Trans. R. Soc. Edinburgh* **104,** 55–67 (2013).
7. Christner, B. C. *et al.* A microbial ecosystem beneath the West Antarctic ice sheet. *Nature* **512,** 310–313 (2014).
8. Skidmore, M. in *Antarctic Subglacial Environments, Geophysical Monograph Series* (eds. Siegert, M. J., Kennicutt II, M. C. & Bindschandler, R. A.) 61–81 (American Geophysical Union, 2011).
9. Fisher, A. T., Mankoff, K. D., Tulaczyk, S. M. & Tyler, S. W. High geothermal heat flux measured below the West Antarctic Ice Sheet. *Sci. Reports* **1,** 1–9 (2015).
10. Whiticar, M. J. Carbon and hydrogen isotope systematics of bacterial formation and oxidation of methane. *Chem. Geol.* **161,** 291–314 (1999).

11. Coleman, D. D., Liu, C.-L. & Riley, K. M. Microbial methane in the shallow Paleozoic sediments and glacial deposits of Illinois, U.S.A. *Chem. Geol.* **71,** 23–40 (1988).
12. Conrad, R. in *Advances in Agronomy* (ed. Sparks, S.) 1–63 (Elsevier, 2007).
13. Schoell, M. Multiple origins of methane in the Earth. *Chem. Geol.* **71,** 1–10 (1988).
14. Michaud, A. B. *et al.* Solute sources and geochemical processes in Subglacial Lake Whillans, West Antarctica. *Geology* **44,** 347–350 (2016).
15. Telling, J. *et al.* Rock comminution as a source of hydrogen for subglacial ecosystems. *Nat. Geosci.* **8,** 851–855 (2015).
16. Lin, L.-H., Slater, G. F., Sherwood Lollar, B., Lacrampe-Couloume, G. & Onstott, T. C. The yield and isotopic composition of radiolytic H_2, a potential energy source for the deep subsurface biosphere. *Geochim. Cosmochim. Acta* **69,** 893–903 (2005).
17. Matheus Carnevali, P. B. *et al.* Methane sources in arctic thermokarst lake sediments on the North Slope of Alaska. *Geobiology* **13,** 181–197 (2015).
18. Lever, M. A. *et al.* Evidence for microbial carbon and sulfur cycling in deeply buried ridge flank basalt. *Science.* **339,** 1305–1308 (2013).
19. Blazewicz, S. J., Barnard, R. L., Daly, R. A. & Firestone, M. K. Evaluating rRNA as an indicator of microbial activity in environmental communities: limitations and uses. *ISME J.* **7,** 2061–2068 (2013).
20. Jones, S. E. & Lennon, J. T. Dormancy contributes to the maintenance of microbial diversity. *Proc. Natl. Acad.* **107,** 5881–5886 (2010).
21. Achberger, A. M. *et al.* Microbial community structure of Subglacial Lake Whillans, West Antarctica. *Front. Microbiol.* **7,** 1–13 (2016).
22. Grant, N. J. & Whiticar, M. J. Stable carbon isotopic evidence for methane oxidation in

plumes above Hydrate Ridge, Cascadia Oregon Margin. *Global Biogeochem. Cycles* **16,** 1–13 (2002).

23. Coleman, D. D., Risatti, J. B. & Schoell, M. Fractionation of carbon and hydrogen isotopes by methane-oxidizing bacteria. *Geochim. Cosmochim. Acta* **45,** 1033–1037 (1981).

24. McDonald, I. R., Bodrossy, L., Chen, Y. & Murrell, J. C. Molecular ecology techniques for the study of aerobic methanotrophs. *Appl. Environ. Microbiol.* **74,** 1305–15 (2008).

25. Knief, C. Diversity and habitat preferences of cultivated and uncultivated aerobic methanotrophic bacteria evaluated based on pmoA as molecular marker. *Front. Microbiol.* **6,** 1346 (2015).

26. Ho, A. *et al.* Conceptualizing functional traits and ecological characteristics of methane-oxidizing bacteria as life strategies. *Environ. Microbiol. Rep.* **5,** 335–345 (2013).

27. Martineau, C., Whyte, L. G. & Greer, C. W. Stable isotope probing analysis of the diversity and activity of methanotrophic bacteria in soils from the Canadian high Arctic. *Appl. Environ. Microbiol.* **76,** 5773–84 (2010).

28. Graef, C., Hestnes, A. G., Svenning, M. M. & Frenzel, P. The active methanotrophic community in a wetland from the High Arctic. *Environ. Microbiol. Rep.* **3,** 466–472 (2011).

29. He, R. *et al.* Shifts in identity and activity of methanotrophs in Arctic lake sediments in response to temperature changes. *Appl. Environ. Microbiol.* **78,** 4715–4723 (2012).

30. Shock, E. L. *et al.* Quantifying inorganic sources of geochemical energy in hydrothermal ecosystems, Yellowstone National Park, USA. *Geochim. Cosmochim. Acta* **74,** 4005–4043 (2010).

31. Amend, J. P. & Shock, E. L. Energetics of overall metabolic reactions of thermophilic and hyperthermophilic Archaea and Bacteria. *FEMS Microbiol. Rev.* **25,** 175–243 (2001).
32. Vick-Majors, T. J. *et al.* Physiological ecology of microorganisms in Subglacial Lake Whillans. *Front. Microbiol.* **7**, 1-16 (2016).
33. Trimmer, M. *et al.* Riverbed methanotrophy sustained by high carbon conversion efficiency. *ISME J.* **9,** 2304–2314 (2015).
34. Iversen, N. & Blackburn, T. H. Seasonal rates of methane oxidation in anoxic marine sediments. *Appl. Environ. Microbiol.* **41,** 1295–1300 (1981).
35. Marlow, J. J. *et al.* Carbonate-hosted methanotrophy represents an unrecognized methane sink in the deep sea. *Nat. Commun.* **5,** 5094 (2014).
36. Bastviken, D., Ejlertsson, J., Sundh, I. & Tranvik, L. Methane as a source of carbon and energy for lake pelagic food webs. *Ecology* **84,** 969–981 (2003).
37. Lough, A. C. *et al.* Seismic detection of an active subglacial magmatic complex in Marie Byrd Land, Antarctica. *Nat. Geosci.* **6,** 1031–1035 (2013).
38. Beem, L. H., Jezek, K. C. & Van Der Veen, C. J. Basal melt rates beneath Whillans Ice Stream, West Antarctica. *J. Glaciol.* **56,** 647–654 (2010).
39. Yvon-Durocher, G. *et al.* Methane fluxes show consistent temperature dependence across microbial to ecosystem scales. *Nature* **507,** 488–91 (2014).

Correspondence and requests for materials should be addressed to A.B.M or J.P.

Acknowledgments

This study was funded by National Science Foundation – Division of Polar Programs

299 grants (0838933, 1346250, 1439774 to J.C.P; 0838941 to B.C.C) awarded as part of the Whillans
300 Ice Stream Subglacial Access Research Drilling (WISSARD) project. We thank the WISSARD
301 Science Team (see wissard.org for full list of team members) for their assistance in expedition
302 planning and with collecting and processing samples. Partial support was provided by graduate
303 fellowships from the NSF-IGERT Program (0654336), Montana Space Grant Consortium and
304 NSF-Center for Dark Energy Biosphere Investigations (A.B.M); a dissertation grant from the
305 American Association of University Women (T.J.V-M); a NSF-Graduate Research Fellowship
306 (A.M.A); and a Sêr Cymru National Research Network for Low Carbon, Energy and the
307 Environment Grant from the Welsh Government and Higher Education Funding Council for
308 Wales (A.C.M). We thank R. Scherer and R. Powell for sediment cores. B.B Jørgensen, M.A.
309 Lever and S. Nielsen provided support and assistance with DNA extraction and *pmoA/mcrA*
310 amplification. Logistics were conducted by the 139th Expeditionary Airlift Squadron of the New
311 York Air National Guard, Kenn Borek Air, and Antarctic Support Contractor, managed by
312 Lockheed-Martin. Hot-water drill support was provided by University of Nebraska-Lincoln and
313 directed by F. Rack and D. Duling (chief driller). D. Blythe, J. Burnett, C. Carpenter, D. Gibson,
314 J. Lemery, A. Melby, and G. Roberts provided drill support at SLW. This is C-DEBI
315 contribution #371.
316

Author Contributions

A.B.M, J.E.D, T.J.V-M, J.C.P and M.L.S wrote the manuscript. A.B.M., J.E.D., M.L.S, and T.J.V-M. conducted and analyzed methane concentration and isotopic data. A.M.A., A.B.M., and B.C.C. processed, analyzed and interpreted the molecular data. A.C.M conducted thermodynamic calculations. All authors contributed to the study design, collection of samples and approved the final draft of the manuscript.

Competing Financial Interests

The authors declare no competing financial interests.

Figure Captions

Figure 1 SLW water column and sediment profile of CH_4 concentration and stable isotope composition and abundance of active methane oxidizing and methanogenic taxa. (**a**) CH_4 concentration and $\delta^{13}C$-CH_4 values, (**b)** percent relative abundance of known CH_4 oxidizing and methanogenic bacterial and archaeal taxa, respectively, from the community analysis of 16S rRNA molecules (note log scale; panel b modified from ref. 21). Dashed lines indicate running averages using a Loess smoothing function (a). SLW water column values for CH_4 concentration and stable isotope values are displayed next to points (a). Asterisks indicate that methanogenic (red) and methanotrophic (black) genera were not detected (b).

Figure 2 CH_4 stable isotope biplot for nine depths of the SLW sediment porewater (black triangles). The shaded areas delineate microbial and thermogenic endmembers as well as regions of mixed sources (endmember fields modified from ref. 10). $\delta^{13}C$-CH_4 values in this plot are the same as Fig. 1A.

Figure 3 Neighbor-joining phylogenetic tree of SLW *pmoA* DNA sequences. *pmoA* sequences from SLW water column and sediment are highlighted in grey and brackets indicate the number of sequenced clones within each operational taxonomic unit (OTU) with sequence accession numbers are shown in parentheses. All solid line branches are *pmoA* sequences of the *Gammaproteobacteria* type Ia group, including *Methylobacter tundripaludum* (bold), an active and abundant member of the SLW community[1,17]. Bootstrap support is displayed at branch points (%, 1000 replications), with values >50% shown. Branch lengths are measured in number of substitutions per site. The scale bar represents 0.05 substitutions per site.

Figure 4 Chemical affinity calculations for the SLW surficial (0-2 cm) sediment. Results are presented in energy density of joules per kg of water (J kg H_2O^{-1}; top axis in log scale) and kilojoules per mole of electron transferred (kJ mol e^{-1}; bottom axis) at 50% (0.5) and 10% (0.1) of the SLW lake water O_2 concentration for eight environmentally relevant biochemical reactions.

Methods

Sample Collection. We used a microbiologically-clean hot water drill to directly sample the water column and the upper 40 cm of sediment of Subglacial Lake Whillans (SLW; 84.240° S, 153.694° W) to assess the CH_4 dynamics[40,41]. SLW water column and sediment were sampled through a 800 m deep, ~0.6 m diameter borehole on 30 January 2013. The clean access hot water drill system has been shown to reduce cell concentrations within the drilling water to <100 cell mL^{-1}, which is acceptable based on the predicted cell concentration in the lake water and the National Research Council 2007 report on subglacial lake access[40,45]. The 2.2 m deep SLW water column was sampled with a 10 L Niskin bottle, suspended microbial cells were concentrated using an *in situ* water filtration system and surficial sediments were collected with a gravity multicorer (60 cm long x 6 cm diameter). For complete drilling and sampling details see ref. 40, 41.

Geochemical Analysis. Sediment from a gravity core (MC-2A) was sampled every 2 cm by extrusion and subsampling of each newly exposed layer. Sediment subsamples for methane (CH_4) were collected using a sterile cut-off 5 ml syringe and immediately placed into 20 ml sterile serum vials and stoppered with a sterile butyl rubber stopper, then crimped with an

aluminum cap. Three empty vials were sealed in the field to capture atmospheric air as procedural blanks. Ten ml of 2.5% NaOH was added by sterile syringe to each sample vial and the three blanks, stopping biological activity and creating a pressurized headspace within each vial[42]. A CH_4 sample from the SLW water column was collected from cast 1 from a Niskin bottle by placing the tube to the bottom of the serum vial and filling from top to bottom. The water sample was fixed with Lugol's solution to prevent biological activity. All vials were stored inverted at 4°C for transport back to Montana State University (MSU) for CH_4 quantification. Headspace CH_4 was quantified on a Hewlett-Packard 5890 Series II gas chromatograph (GC) equipped with a flame ionization detector (FID) with a detection limit of 3 nM for water column samples and 190 nM for the sediment samples. Headspace gas was introduced to the GC using a 10-port injection valve configured for back flushing of a precolumn (25 cm x 0.32 cm OD, packed with Porapak-T 80/100 mesh) to prevent water vapor from reaching the analytical columns. The vial overpressure was used to flush and fill a 1 cm^3 sample loop using a syringe needle inlet; measured laboratory air temperature and pressure were used to calculate the total moles of gas contained within the loop, assuming gas ideality. Gases were separated on two analytical columns in series (both 183 cm x 0.32 cm OD, packed with Chromosorb 102 80/100 mesh and Porapak-Q 80/100 mesh, respectively). The columns were maintained at 55°C and the FID at 240°C. The carrier gas was an ultra-high purity N_2, which was further purified through Molecular Sieve 5A, activated charcoal and an O_2 scrubber. The carrier flow was 30 mL min^{-1}; under these conditions, CH_4 eluted to the FID at 1.97 min. Instrument calibration was performed using certified 500 and 51 ppmv CH_4 in air standards (Air Liquide; ±1% accuracy), and volumetric dilutions thereof into carrier N_2. Dissolved CH_4 concentrations were calculated using Henry's Law based on measured headspace mole fractions and Bunsen solubility coefficients

396 estimated from temperature and sample salinity (including added NaOH) as parameterized by
397 ref. 46. Porewater volumes were determined from mass loss after drying the sediment at 95°C
398 until the mass stopped decreasing (~24h), and dry sediment volume was similarly determined
399 assuming a density of 2.60 g cm^{-3} for the sedimentary particles[47]. The total volume of the vials
400 was determined weighing the vials with sediment and NaOH fixative, then completely filling the
401 headspace with deionized water and weighing again. The headspace volume was determined by
402 difference. The extent of pressurization of the headspace was determined from total headspace
403 volume and the volume of NaOH solution added. The total CH_4 within each vial, after correction
404 for the small amount of CH_4 present in the headspace air when originally sealed (characterized
405 by the blank vials), was then used to determine the initial CH_4 concentration of the porewater.
406 Gravity core MC-3A was collected from SLW, capped and immediately frozen (-20°C).
407 The frozen core was returned to MSU and thawed at 4°C overnight in a class 1000 clean, cold
408 room in the MSU SubZero Science and Engineering Facility. The core was extruded and cut
409 every 2 cm and sediment for CH_4 stable isotope analysis was subsampled and fixed using the
410 same method as for CH_4 concentration analysis from MC-2A described above. One ml of room
411 temperature headspace gas from the fixed sediment vials was transferred to a gas-tight laminated
412 foil bag using a gas-tight, glass syringe and diluted 1:100 with CH_4-free (zero grade) air. The bag
413 was connected to the inlet of a Picarro G2201-*i* Cavity Ring-Down Spectrometer (CRDS)
414 specific for high-precision concentration and $\delta^{13}C$ analyses of CH_4. Sample was introduced to
415 the instrument at a flow rate of 100 ml min^{-1}; $\delta^{13}C$-CH_4 values were determined using factory
416 calibrations and were averaged over ≥30 s of 1 Hz measurements. Between samples, atmospheric
417 air was measured for at least 5 min to ensure lack of instrument drift. The δD-CH_4 values were
418 measured at the University of California Davis Stable Isotope Facility (UCD-SIF) using a

PreCon concentration system (ThermoScientific) in line with a Delta V plus isotope ratio mass spectrometer (ThermoScientific)[43]. Two $\delta^{13}C$-CH_4 samples (MC-3A samples from 18-20 cm and 34-36 cm depths) were also run at UCD-SIF to compare their independent results with our values obtained on the Picarro CRDS. There was a <4% difference in the $\delta^{13}C$-CH_4 values reported from the two methods. The carbon and hydrogen stable isotope ratios are reported in δ-notation ($\delta^{13}C$, δD) with respect to VPDB and VSMOW standards, respectively. The running average (with depth) of the CH_4 concentration and isotope values was calculated in SigmaPlot version 11 using a locally estimated scatterplot smoothing (loess) function with smoothing parameters set to first degree polynomial and a sampling frequency of 0.45, which determines the number of local data points used in the weighted regression carried out by the loess smoothing function.

Sediments used for dissolved NH_4^+ concentration measurements were collected from MC-3A[48]. The sediment was transferred to acid washed (10% HCl), ultra-pure water-rinsed (6X), combusted (4h at 450 °C) glass vials with polytetrafluoroethylene lined caps, frozen at -20 °C and thawed prior to analysis. Sediments were transferred from the glass vials to acid washed and ultra-pure water rinsed 50 mL conical centrifuge tubes and centrifuged at 3500 x g for 20 minutes. The supernatant was transferred to acid washed and ultra-pure water rinsed 15 ml conical centrifuge tubes and spun for an additional 20 min at 4500 x g to pellet fine particulates. The clean supernatant from the 15 mL centrifuge tube was transferred to an acid washed and ultra-pure water rinsed glass vial. The supernatant was diluted (1:10) to a final volume of 5 mL with ultra-pure water for colorimetric analysis[49].

Particulate organic carbon and nitrogen values were determined with an elemental analyzer as described in ref 1. Acetate, formate and oxalate concentrations were determined using ion chromatography following methods in ref. 14.

442 **Molecular Analyses.** DNA was extracted using a modular method to allow for
443 optimization of the DNA extraction procedure, specific to the SLW sediments[44]. DNA extraction
444 yield from SLW sediments was greatest when sediments were pre-treated with 450 μmol g^{-1}
445 deoxynucleotide triphosphate to prevent adsorption of lysed DNA to the abundant clay particles
446 in SLW[44]. The particulate methane monooxygenase (*pmoA*) gene clone libraries were
447 constructed by PCR amplification using A189F (5' GGNGACTGGGACTTCTGG 3') and
448 m680R (5' CCGGMGCAACGTCYTTACC 3')[24]. The PCR was set up using 0.13 μL of ExTaq
449 at 5 units μL^{-1} (Takara), 2.5 μL of 10x ExTaq buffer (Takara), 2 μL dNTP mixture at 2.5mM per
450 nucleotide (Takara), 2.5 μL of A189F and Mb661R primers (10 pmol μL^{-1}), 2 μL molecular
451 biology-grade bovine serum albumen (BSA; 1.6 mg ml^{-1} final concentration) (New England
452 BioLabs Inc.), 4 μL of template DNA (0.01-0.09 ng DNA μL^{-1}), and 11.37 μL of PCR-grade
453 water for a final reaction volume of 25 μL. The PCR thermocycling conditions were 1 cycle of
454 98°C for 2 min; 40 cycles of 98°C for 15 s, 55°C for 1 min, and 72°C for 1 min; followed by a
455 final 72°C for 7 min. PCR was conducted with DNA extraction blanks and no template blanks
456 (PCR-grade water) as negative controls. Negative controls were not carried forward for cloning,
457 as no PCR bands were detected. PCR products were run on a 1.5% agarose gel and the 491
458 basepair *pmoA* fragment was excised from the gel with sterile razor blade and DNA was purified
459 using a Wizard SV gel clean-up system (Promega). Cleaned *pmoA* fragments were immediately
460 ligated and cloned with a TA Cloning kit (Invitrogen). Positive clones were transferred to
461 LB+ampicillin broth and grown overnight at 37°C, then sequenced (288 total sequenced clones)
462 (Functional Bioscience). The *pmoA* DNA sequences were processed by removing the forward
463 and reverse primer sequences and removing poor quality sequences (<20 phred score)[50]. Quality
464 controlled *pmoA* sequences (176 total) were clustered into operational taxonomic units (OTUs) at

465 the 97% similarity level and one representative sequence from each OTU[51], along with
466 representative *pmoA* sequences from type Ia and II methanotrophs[24], were aligned using
467 ClustalW using the default alignment parameters within the program MEGA6[52]. A phylogenetic
468 tree was built using the neighbor-joining method with 1000 bootstrap replications[52]. The *pmoA*
469 sequences have been deposited in GenBank under accession numbers KX589304-KX589461 and
470 KX784213-KX84230.

471 We attempted to amplify *mcrA* gene sequences from SLW sediment DNA extracts using
472 a primer set designed to amplify the diversity of *mcrA*-containing methanogens[18] with a nested
473 PCR amplification scheme. The primer pair used to detect the *mcrA* gene sequence were mcrIRD
474 [18]. The primer pair is capable of detecting a wide diversity of known and several novel *mcrA*
475 gene clusters[18]. The first reaction was set up using 0.13 µL of Takara ExTaq at 5 units μL^{-1}, 2.5
476 µL 10x ExTaq buffer, 2 µL dNTP mixture at 2.5mM per nucleotide (Takara), 2.5 µL of forward
477 and reverse primer (10 pmol μL^{-1}), 2 µL of BSA (1.6 mg ml^{-1} final concentration), 9.38 µL PCR-
478 grade water and 4 µL DNA extract (0.01-0.09 ng DNA μL^{-1}) for a final reaction volume of 25
479 µL. This first reaction was run with an initial denaturation step at 98°C for 2 minutes followed
480 by 40 cycles of 98°C for 15 s, 53°C for 1 min and 72°C for 1 min, and a final elongation at 72°C
481 for 7 min. The second reaction was set up using 0.25 µL Takara ExTaq, 5 µL 10x ExTaq buffer,
482 4 µL dNTP mixture at 2.5mM per nucleotide (Takara), 5 µL of forward and reverse primers (10
483 pmol μL^{-1}), 4 µL of BSA (1.6 mg ml^{-1} final concentration), 21.75 µL of PCR-grade water and 4
484 µL of product from the first reaction as template DNA. The second reaction was run with the
485 same thermocycler program as the first reaction. PCR was conducted with DNA extraction
486 blanks and no template blanks (PCR-grade water) as negative controls. Details of the 16S rRNA
487 molecule sample collection and preservation, extraction, reverse transcription, sequencing and

488 processing are described in ref. 21. Extraction blanks were conducted, processed and analyzed in
489 parallel with the SLW sediment samples as described in ref. 21.

490 **Chemical Affinity Calculations.** An assessment of CH_4 as a potential chemical energy
491 source for the surficial (0-2 cm) sediment layer was undertaken. The chemical affinity of coupled
492 oxidation-reduction reactions involving CH_4 and other potential metabolic reactions was
493 determined. The chemical affinity (A_r) is the maximum amount of energy that can be obtained
494 for a reaction based on *in situ* conditions. A_r is defined as the change in the overall Gibbs energy
495 under non-equilibrium conditions (ΔG_r^o) with a change in the progress of the reaction, which
496 quantifies the reactions proximity to equilibrium[30,31] and is given by;

497 $$A_r = RT \ln(K_r/Q_r) \quad \text{(S1)}$$

498 where, K_r is the calculated equilibrium constant for the reaction, which is derived from ΔG_r^o of
499 the reaction according to $\Delta G_r^o = G_f^o$ products - G_f^o reactants, where G_f^o is the standard Gibbs
500 energy of formation for the products and reactants[53]. K_r is given by;

501 $$K_r = e^{-\Delta G_r{}^o/RT} \quad \text{(S2)}$$

502 where R is the gas constant 0.008314 kJ mol^{-1}, and T is SLW temperature in Kelvin [-0.5°C =
503 272.65 K][53]. Thermodynamic values were derived from ref. 31 using values for 2°C, the closest
504 available values for the temperature of SLW (-0.5°C); the impact of the temperature difference
505 on ΔG_r^o and resulting K_r values will be small[30,31].

506 Q_r is the activity product for the reaction, determined as;

507 $$Q_r = \prod_i (a_i)^{Vi,r} \quad \text{(S3)}$$

508 where a_i represents the activity of the i^{th} compound in the reaction raised to its stoichiometric
509 coefficient in the r^{th} reaction, $v_{i,r}$, which is positive for products and negative for reactants.
510 Activities are calculated from molal concentrations (m_i) using activity coefficients (γ_i) and the

relationship $a_i = m_i\gamma_i$[30]. These activities were calculated using the geochemical model PHREEQCi[54] using the empirical SLW geochemistry[7,14]. The O_2 concentration in the 0-2 cm layer was not measured, but for the chemical affinity calculations we consider two scenarios of O_2 concentration set at 50% (36.5 μM) and 10% (7.3 μM) of average SLW lake water to account for the decrease in sedimentary O_2 concentration due to consumption and diffusion[55]. Given that oxygen is inferred to penetrate to ~16cm based on redox sensitive trace metal concentrations[14], it is reasonable to model chemical affinity using these two concentrations of O_2 in the surficial sediment. Temperature, pH, redox (pE) and concentrations of acetate, formate (Supplementary Fig. 1), dissolved inorganic carbon (DIC), O_2(aq), CH_4(aq), SO_4^{2-}, NO_3^-, NH_4^+, total dissolved Fe, Ca^{2+}, Mg^{2+}, Na^+, K^+, P, Li^+, Br^-, Cl^- and F^- were defined[7,14,32,48]. Redox sensitive elements that were measured as total dissolved elemental concentration (i.e. C, Fe) were assumed to be speciated to the redox states and species activities as determined by PHREEQC. Conversely, ions measured in specific redox states (i.e. SO_4^{2-}, NO_3^-, NH_4^+) were maintained in their respective redox states by the model, and the species activities including these ions were calculated.

The chemical affinities are expressed in per electron yields ($A_r^{e^-}$) and also shown in terms of energy density, the energy per kg H_2O (A_r^{kg}), which scales the energy availability to the limiting reactant, calculated as;

$$A_r^{kg} = \left|\frac{A_r}{v_i}\right| [i] \quad \text{(S4)}$$

where, $[i]$ refers to the concentration of the limiting electron donor or acceptor[56]. This scaling [equation (S4)] of chemical affinity has been shown to better correlate with actual microbial communities and metabolisms than the chemical affinity normalized to moles of electrons transferred[56,57].

Methane Oxidation Rate Modeling. CH_4 oxidation rates were modeled by calculating the flux of CH_4 into the 0-2 cm sediment layer. The CH_4 concentration gradient was determined using CH_4 values from 15 cm to 3 cm. The flux was calculated using Fick's first law and the error of the flux determined from the error associated with the diffusional gradient. Water content was measured and calculated by weighing a known volume of wet weight sediment, then measuring the sediment again after drying at 95°C for three days[42,47]. Porosity was calculated from the water content and density of the sediment[42,47]. The diffusion coefficient for CH_4 at 0°C was corrected for porosity (Supplementary Fig. 3) and tortuousity of SLW sediments calculated according to equation 3.11 from ref. 58 with C=2.02[58,59]. We modeled the rate of biological CH_4 consumption according to equation (1) (See main text).

The control volume of our model can be defined by the relationship;

$$V = A \times H_L + (H_{SS} \times \varphi) \quad \text{(S5)}$$

where, H_L and H_{SS} are the height of the lake and surficial sediments, respectively, and φ is the sediment porosity. Assuming steady-state conditions (i.e., $\frac{dC}{dt} = 0$) and substitution of equation (S5) into equation (1), R can be calculated as shown in equation (2). R represents the sum of both microbial CH_4 oxidation to CO_2 and incorporation of CH_4 into biomass. We estimated the amount of CH_4 removal due to oxidation and incorporation of biomass by assuming that the biomass partitioning factor, of CH_4 going to biomass is 0.5 [x; equation (S6)]. The value of 0.5 has been shown to be a good approximation for the fraction of biomass incorporated by type I methanotrophs during CH_4 oxidation and is a median value across many habitats[33,60,61]. We calculated the impact of varying x from 0.06 to 0.77[36] on biomass C production and methanotrophy oxygen demand (Supplementary Table 1). From the CH_4 removal rate and the

fraction of CH_4 incorporated into biomass, we can then calculate the O_2 consumption by CH_4 oxidation, which follows the stoichiometric relationship:

$$CH_4 + (2 - x)O_2 \rightarrow (1 - x)CO_2 + xCH_2O + (2 - x)H_2O \quad \text{(S6)}$$

where *x* is the fraction of CH_4 partitioned into biomass formation[33,60,62]. The inputs of O_2 to the lake are from atmospheric gases released by melting of the overlying meteoric ice and advection of water into the lake during the filling phase of the hydrologic cycle[9,32,63]. Based on the concentration of gas in the overlying ice and the basal ice melt rate, which has been estimated at 1.8 cm y^{-1} (ref. 9), the overlying ice sheet supplies 1.0 x 10^6 mol O_2 yr^{-1} (67% of O_2 supply to SLW)[32]. Advection into the lake provides 5 x 10^5 mol O_2 yr^{-1} (33% of O_2 supply to SLW)[32], assuming the incoming water has the same concentration measured in the SLW water column[32,63]. When the fraction of carbon from CH_4 going to biomass is varied (Supplementary Table 1), the oxygen demand on the system changes as well. We used the SLW oxygen budget from ref. 32 to determine the impact of the biomass partitioning factor (*x*) could have on the oxygen demand for biological processes in SLW (Supplementary Table 1).

Data availability. Data generated for this study are available through the microbial Antarctic resource system database (http://mars.biodiversity.aq/resources/97). Molecular data were accessed from NCBI sequence read archive (https://www.ncbi.nlm.nih.gov/sra) project PRJNA244335.

References

40. Priscu, J. C. *et al.* A microbiologically clean strategy for access to the Whillans Ice Stream subglacial environment. *Antarct. Sci.* **11,** 1–11 (2013).

41. Tulaczyk, S. *et al.* WISSARD at Subglacial Lake Whillans, West Antarctica: scientific

operations and initial observations. *Ann. Glaciol.* **55,** 51–58 (2014).

42. Riedinger, N. *et al.* Methane at the sediment–water transition in Black Sea sediments. *Chem. Geol.* **274,** 29–37 (2010).

43. Yarnes, C. ^{13}C and ^{2}H measurement of methane from ecological and geological sources by gas chromatography/combustion/pyrolysis isotope-ratio mass spectrometry. *Rapid Commun. Mass Spectrom.* **27,** 1036–1044 (2013).

44. Lever, M. A. *et al.* A modular method for the extraction of DNA and RNA, and the separation of DNA pools from diverse environmental sample types. *Front. Microbiol.* **6,** 1–25 (2015).

45. National Resource Council. *Exploration of Antarctic Subglacial Aquatic Environments*. (The National Academies Press, 2007).

46. Wiesenburg, D. A. & Guinasso Jr., N. L. Equilibrium solubilities of methane, carbon monoxide, and hydrogen in water and sea water. *J. Chem. Eng. Data* **24,** 356–360 (1979).

47. Avnimelech, Y., Ritvo, G., Meijer, L. E. & Kochba, M. Water content, organic carbon and dry bulk density in flooded sediments. *Aquac. Eng.* **25,** 25–33 (2001).

48. Vick-Majors, T. J. Biogeochemical processes in Antarctic aquatic environments: Linkages and limitations. (Montana State University, 2016).

49. Solorzano, L. Determination of ammonia in natural waters by the phenolhypochlorite method. *Limnol. Oceanogr.* **14,** 799–801 (1969).

50. Paegel, B. M., Emrich, C. A., Wedemayer, G. J., Scherer, J. R. & Mathies, R. A. High throughput DNA sequencing with a microfabricated 96-lane capillary array electrophoresis bioprocessor. *Proc. Natl. Acad. Sci.* **99,** 574–579 (2002).

51. Schloss, P. D. *et al.* Introducing mothur: Open-source, platform-independent, community-

supported software for describing and comparing microbial communities. *Appl. Environ. Microbiol.* **75,** 7537–7541 (2009).

52. Tamura, K., Stecher, G., Peterson, D., Filipski, A. & Kumar, S. MEGA6: Molecular evolutionary genetics analysis version 6.0. *Mol. Biol. Evol.* **30,** 2725–2729 (2013).

53. Stumm, W. & Morgan, J. J. *Aquatic Chemistry: Chemical Equilibria and Rates in Natural Waters*. (Wiley-Interscience, 1996).

54. Parkhurst, D. L. & Appelo, C. A. J. in *U.S. Geological Survey Techniques and Methods* 497 (US Geological Survey, 2013).

55. Boetius, A. & Wenzhöfer, F. Seafloor oxygen consumption fuelled by methane from cold seeps. *Nat. Geosci.* **6,** 725–734 (2013).

56. LaRowe, D. E. & Amend, J. P. in *Microbial Life of the Deep Biosphere* (eds. Kallmeyer, J. & Wagner, D.) 279–302 (Walter de Gruyter, 2014).

57. Osburn, M. R. *et al.* Chemolithotrophy in the continental deep subsurface: Sanford Underground Research Facility (SURF), USA. *Front. Microbiol.* **5,** 1–14 (2014).

58. Shen, L. & Chen, Z. Critical review of the impact of tortuosity on diffusion. *Chem. Eng. Sci.* **62,** 3748–3755 (2007).

59. Broecker, W. S. & Peng, T.-H. Gas exchange rates between air and seal. *Tellus* **26,** 21–35 (1974).

60. Shelley, F., Abdullahi, F., Grey, J. & Trimmer, M. Microbial methane cycling in the bed of a chalk river: oxidation has the potential to match methanogenesis enhanced by warming. *Freshw. Biol.* **60,** 150–160 (2015).

61. Whalen, S. C., Reeburgh, W. S. & Sandbeck, K. A. Rapid Methane Oxidation in a Landfill Cover Soil. *Appl.Environ.Microbiol.* **56,** 3405–3411 (1990).

62. Urmann, K., Lazzaro, A., Gandolfi, I., Schroth, M. H. & Zeyer, J. Response of methanotrophic activity and community structure to temperature changes in a diffusive CH/O counter gradient in an unsaturated porous medium. *FEMS Microbiol. Ecol.* **69,** 202–12 (2009).

63. Siegfried, M. R., Fricker, H. A., Carter, S. P. & Tulaczyk, S. Episodic ice velocity fluctuations triggered by a subglacial flood in West Antarctica. *Geophys. Res. Lett.* **43,** 2640–2648 (2016).

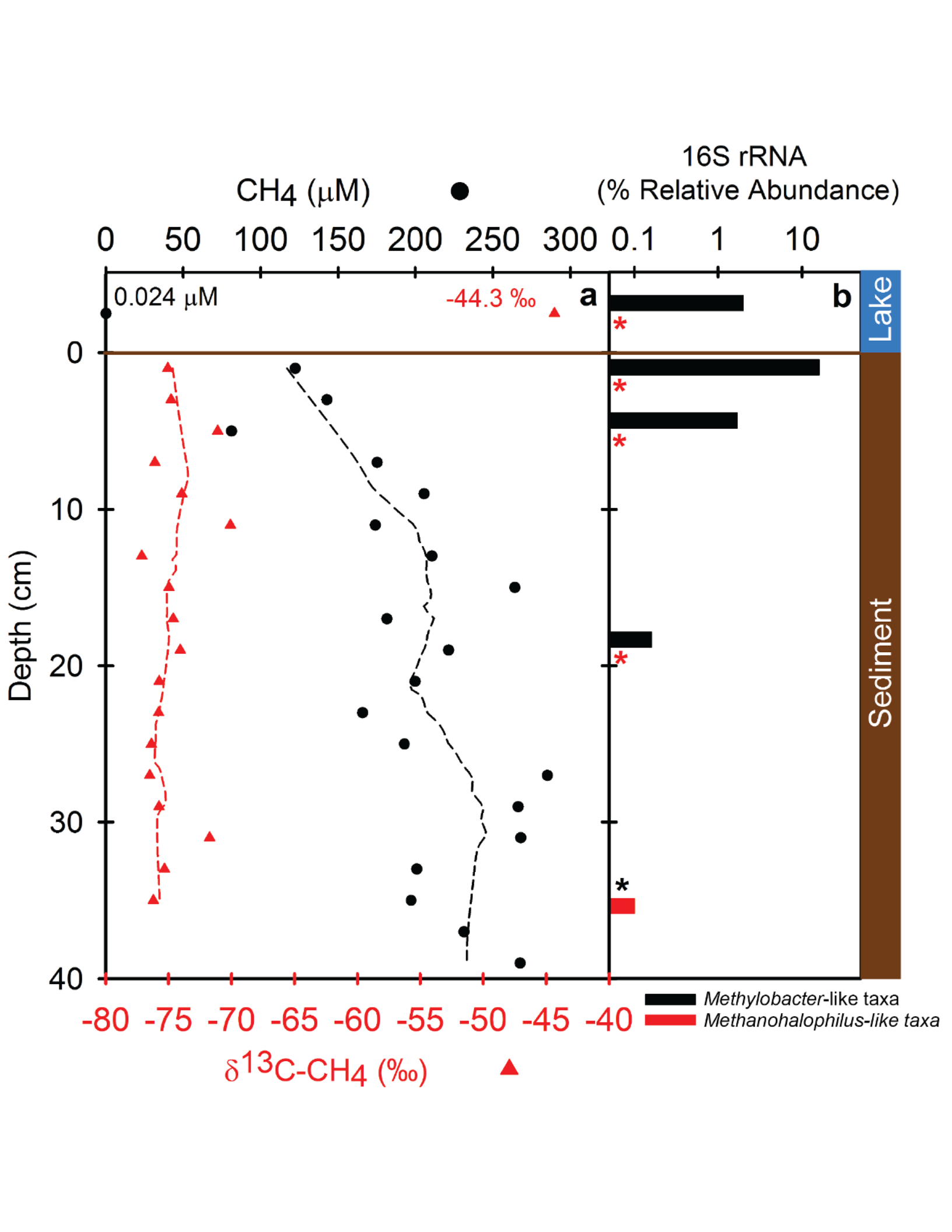
16S rRNA
(% Relative Abundance)
CH4 (μM)
0 50 100 150 200 250 300
0.1 1 10
0.024 μM
-44.3 ‰
a
b
Lake
Sediment
Depth (cm)
0
10
20
30
40
-80 -75 -70 -65 -60 -55 -50 -45 -40
δ13C-CH4 (‰)
Methylobacter-like taxa
Methanohalophilus-like taxa

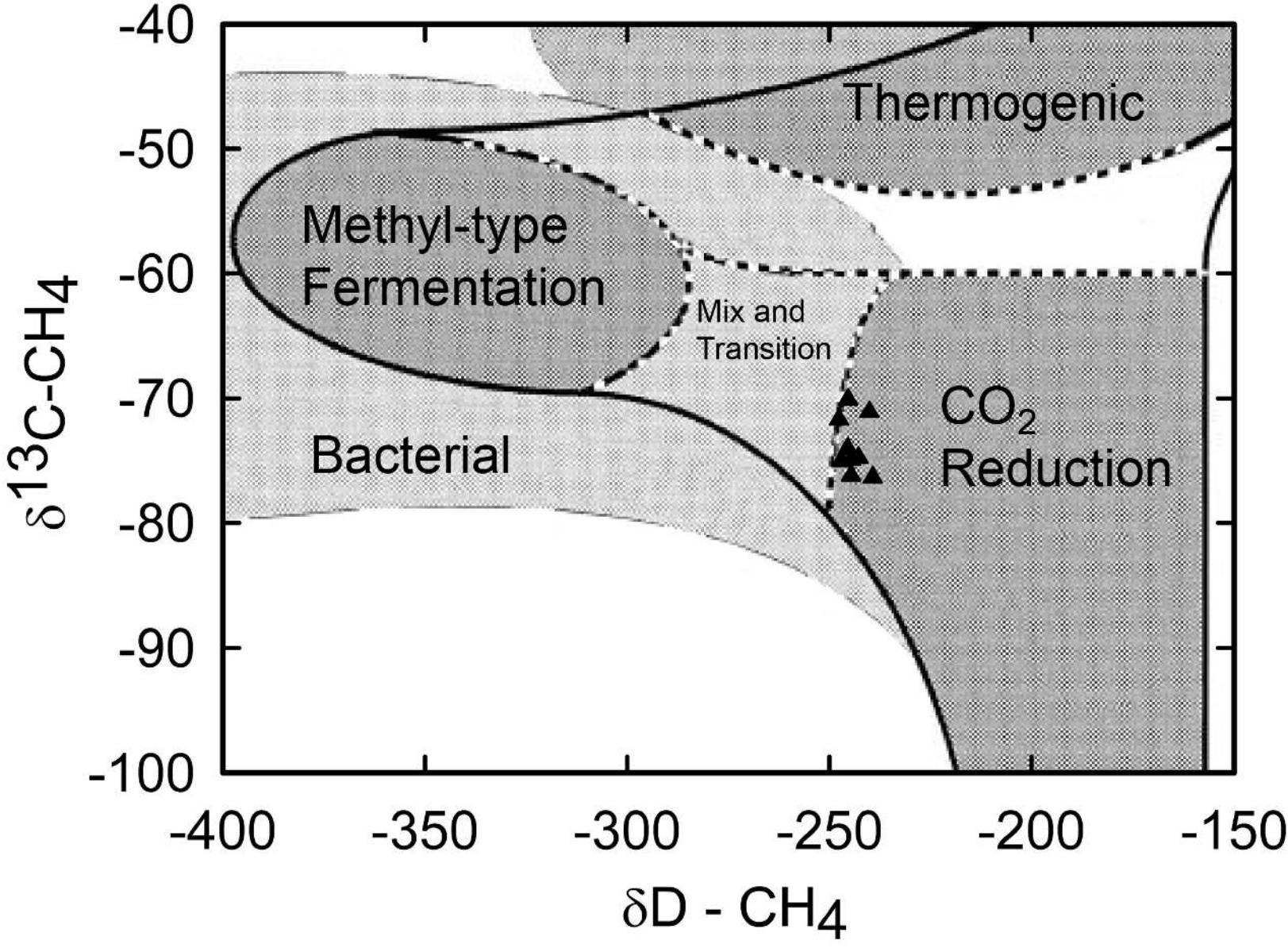
-40
-50
-60
-70
-80
-90
-100
$\delta^{13}C\text{-}CH_4$
Thermogenic
Methyl-type
Fermentation
Mix and
Transition
Bacterial
CO_2
Reduction
-400
-350
-300
-250
-200
-150
$\delta D - CH_4$

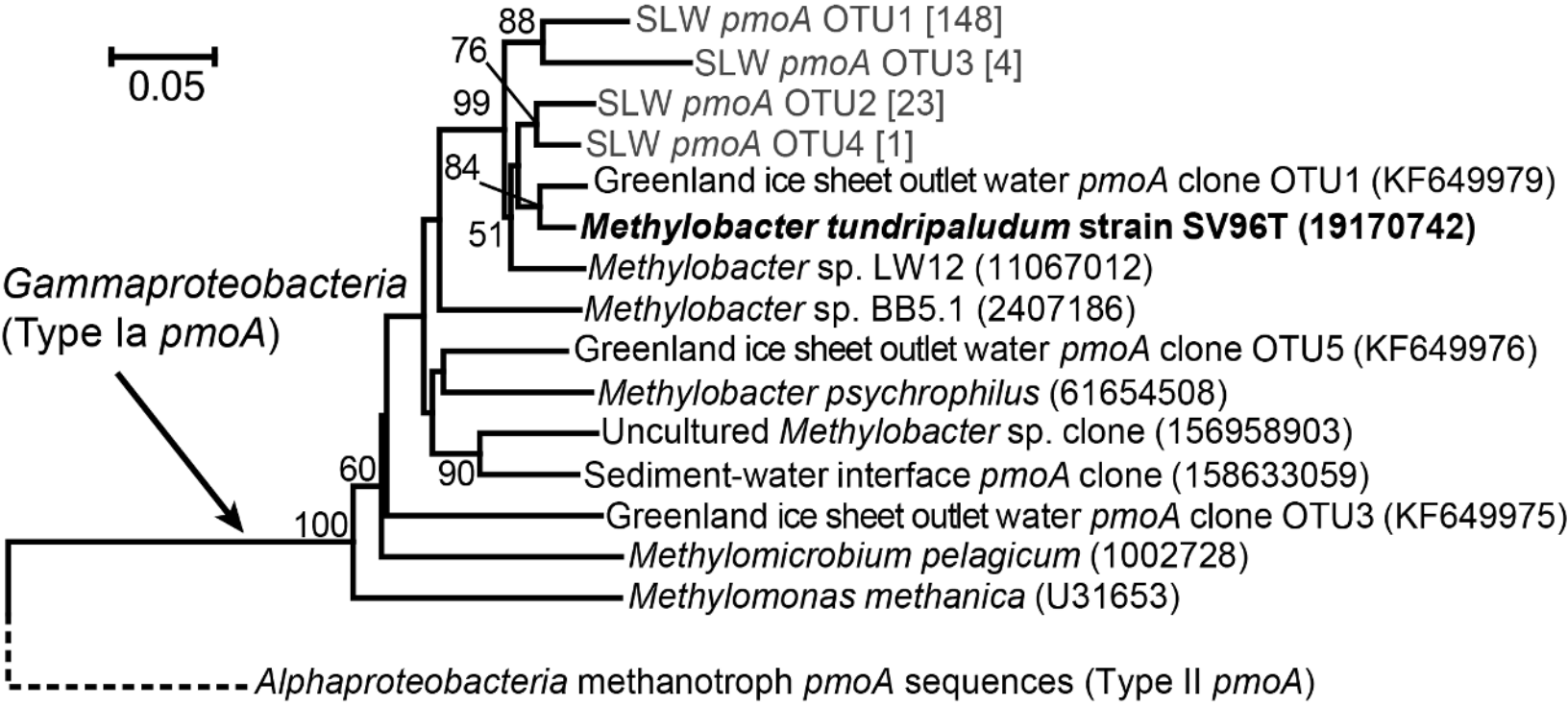
0.05
88
76
99
84
51
60
90
100
SLW pmoA OTU1 [148]
SLW pmoA OTU3 [4]
SLW pmoA OTU2 [23]
SLW pmoA OTU4 [1]
Greenland ice sheet outlet water pmoA clone OTU1 (KF649979)
Methylobacter tundripaludum strain SV96T (19170742)
Methylobacter sp. LW12 (11067012)
Methylobacter sp. BB5.1 (2407186)
Greenland ice sheet outlet water pmoA clone OTU5 (KF649976)
Methylobacter psychrophilus (61654508)
Uncultured Methylobacter sp. clone (156958903)
Sediment-water interface pmoA clone (158633059)
Greenland ice sheet outlet water pmoA clone OTU3 (KF649975)
Methylomicrobium pelagicum (1002728)
Methylomonas methanica (U31653)
Gammaproteobacteria
(Type Ia pmoA)
Alphaproteobacteria methanotroph pmoA sequences (Type II pmoA)

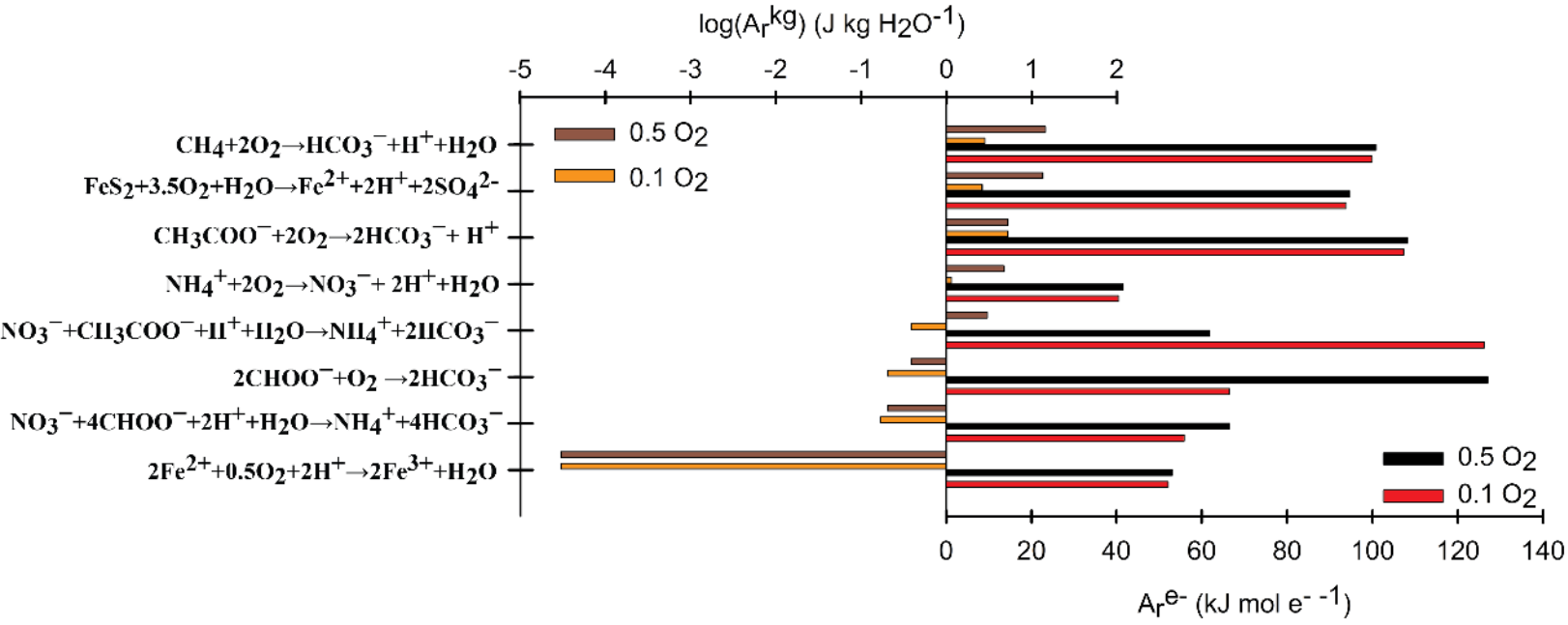
log(Ar^kg) (J kg H2O^-1)
-5
-4
-3
-2
-1
0
1
2
0.5 O2
0.1 O2
CH4+2O2→HCO3−+H+H2O
FeS2+3.5O2+H2O→Fe2++2H++2SO42-
CH3COO−+2O2→2HCO3−+ H+
NH4++2O2→NO3−+ 2H++H2O
NO3−+CH3COO−+H++H2O→NH4++2HCO3−
2CHOO−+O2 →2HCO3−
NO3−+4CHOO−+2H++H2O→NH4++4HCO3−
2Fe2++0.5O2+2H+→2Fe3++H2O
0.5 O2
0.1 O2
0
20
40
60
80
100
120
140
Ar^e- (kJ mol e- -1)